DOI: 10.1002/ejic.200601196

Ruthenium(II) Complexes of Thiosemicarbazones: The First Water-Soluble Complex with pH-Dependent Antiproliferative Activity

Sanja Grguric-Sipka,[a][‡] Christian R. Kowol,[a] Seied-Mojtaba Valiahdi,[a] Rene Eichinger,[a] Michael A. Jakupec,[a] Alexander Roller,[a] Sergiu Shova,[a][‡‡] Vladimir B. Arion,*[a] and Bernhard K. Keppler*[a]

Keywords: Antitumour agents / Ruthenium / N,S ligands / X-ray diffraction

Two ruthenium(II) complexes of 2-acetylpyridine N^4,N^4-dimethylthiosemicarbazone (HL^1) and phenanthrenequinone thiosemicarbazone (HL^2), namely $[Ru^{II}Cl(L^1)(PPh_3)_2]$ (**1**) and $[Ru^{II}Cl(L^2)(PPh_3)_2]$ (**2**), have been synthesised and characterised by IR, UV/Vis and NMR spectroscopy, electrospray mass spectrometry, cyclic voltammetry and X-ray crystallography. In addition, the X-ray crystal structure of $[Ru^{III}Cl_2(L^2)PPh_3]$·dmso·$1.25H_2O$ (**3**·dmso·$1.25H_2O$) is reported. The reaction of $[Ru^{II}Cl_2(dmso)_4]$ with HL^1 and 1,3,5-triaza-7-phosphaadamantane (PTA) gives the highly water-soluble complex $[Ru^{II}Cl(L^1)(HPTA)_2]Cl_2$·$C_2H_5OH$·$H_2O$ (**4**·C_2H_5OH·H_2O) ($S_{25°C} \geq 250$ mg/mL), which has been fully characterised. Complex **4** shows strong antiproliferative effects in low micromolar concentrations in the ovarian carcinoma cell line 41M (IC_{50} = 0.87 μM) and more moderate activity in the breast cancer cell line SK-BR-3 (IC_{50} = 39 μM). The activity of the compound is 6.5- and 5.4-times higher at pH = 6.0 than at pH = 7.4 in the non-small cell lung cancer cell line A549 and the colon carcinoma cell line HT-29 (GI_{50} = 24 and 8.0 μM at pH = 6.0 for A549 and HT-29, respectively).

Introduction

Thiosemicarbazones form a class of mixed hard-soft oxygen/nitrogen-sulfur chelating ligands that show a variety of coordination modes in metal complexes. The thiosemicarbazone can act as a monodentate ligand that binds to the metal ion through the sulfur atom[1] or as a bidentate ligand that coordinates to the metal ion through the sulfur atom and one of the nitrogen atoms of the hydrazine moiety to form a four- or a five-membered metallacycle.[2,3] The coordination capacity of thiosemicarbazones can be increased by using for their preparation aldehydes or ketones containing additional functional group(s) in position(s) suitable for chelation.[4] Beside their interesting coordination chemistry, thiosemicarbazones have a wide pharmacological spectrum of activity; their potential has been recognised to include antitumour, antiviral, antibacterial, antifungal and antimalarial properties.[5] The enzyme ribonucleotide reductase has been identified as a principal target, and thiosemicarbazones are among the most potent known inhibitors of this enzyme.[6,7] The inhibition of ribonucleotide reductase prevents the conversion of ribonucleotides into deoxyribonucleotides, which results in the impairment of DNA synthesis and repair.[8] The applicability of thiosemicarbazones as antitumour agents has been explored for over half a century,[9] the first compound of this class to enter phase II clinical trials as an antineoplastic agent being 3-aminopyridine-2-carboxaldehyde thiosemicarbazone (3-AP, triapine).[10,11] The effect of certain metals on the biological activity of thiosemicarbazones has been receiving considerable attention recently.[12–14] Although a large number of reports are available on the chemistry and biological activity of copper(II), cobalt(III), gallium(III), iron(III), platinum(II) or palladium(II) thiosemicarbazonates,[15–18] there are only a few reports on antitumour activity of the corresponding ruthenium complexes.[19,20] Interest in ruthenium was stimulated by phase I clinical trials of two ruthenium complexes, namely (H_2im)[*trans*-$Ru^{III}Cl_4$(Him)(dmso)] (NAMI-A; Him = imidazole) and (H_2ind)[*trans*-$Ru^{III}Cl_4(Hind)_2$] (KP1019; Hind = indazole), the first as an antimetastatic drug and the second as an anticancer agent against primary tumours and metastases, and in particular colon carcinomas.[21,22]

The very high cytotoxicity of our recently synthesised gallium(III) and iron(III) complexes with N^4-substituted α-N-heterocyclic thiosemicarbazones[23] in vitro together with the above-mentioned interest in ruthenium chemistry prompted us to synthesise novel ruthenium complexes of

[a] Institute of Inorganic Chemistry, Faculty of Chemistry, University of Vienna,
Waehringer Str. 42, 1090 Vienna, Austria
Fax: +43-1427752680
E-mail: vladimir.arion@univie.ac.at
bernhard.keppler@univie.ac.at
[‡] On sabbatical leave from the Faculty of Chemistry of the University of Belgrade.
[‡‡] On sabbatical leave from the Department of Chemistry of the Moldova State University.
Supporting information for this article is available on the WWW under http://www.eurjic.org or from the author.

thiosemicarbazones. We chose two ligands, 2-acetylpyridine N^4,N^4-dimethylthiosemicarbazone (HL^1), which shows very high cytotoxicity in the low nanomolar range and the ability to destroy the tyrosyl radical of mouse ribonucleotide reductase R2 protein,[23] and phenanthrenequinone thiosemicarbazone (HL^2), which is known to have antiproliferative activity in the low micromolar range.[24] The presence of the phenanthrene moiety in HL^2 renders this ligand capable of DNA intercalation in addition to its potential ribonucleotide reductase inhibiting properties.

Ruthenium(II) complexes with two monoanionic tridentate thiosemicarbazones are neutral species that are sparingly soluble or even insoluble in aqueous media.[25] Water solubility is required to assay the cytotoxicity in vitro, therefore we focused on the synthesis of complexes with a 1:1 metal/ligand stoichiometry. A literature survey showed that phosphorus-containing species and, in particular, triphenylphosphane often serve as ancillary ligands to complete the coordination sphere of ruthenium upon coordination of a thiosemicarbazone.[26–28] This prompted us to consider 1,3,5-triaza-7-phosphaadamantane (PTA) as a co-ligand as it is known to endow metal complexes with aqueous solubility and solubility in polar organic solvents.[29a–29e,30] The (PTA)ruthenium compounds reported so far that show antiproliferative activity are organometallic compounds derived from [Ru(η^6-*p*-cymene)Cl_2(PTA)],[29a] some of which have been found to cause pH-dependent DNA damage.

Herein we report on the synthesis, spectroscopic characterisation and X-ray diffraction structures of three novel complexes and the pH-dependent in vitro antiproliferative activity of the first thiosemicarbazone/PTA mixed ruthenium(II) complex with high aqueous solubility.

Results and Discussion

The reaction of [$Ru^{II}Cl_2(PPh_3)_3$] with either 2-acetylpyridine N^4,N^4-dimethylthiosemicarbazone (HL^1) in dry dichloromethane or phenanthrenequinone thiosemicarbazone (HL^2) in absolute ethanol afforded the complexes *trans*-[$Ru^{II}Cl(L^1)(PPh_3)_2$] (**1**) and *trans*-[$Ru^{II}Cl(L^2)(PPh_3)_2$] (**2**) in 41 and 80% yield, respectively. In one case the synthesis of **2** was accompanied by marginal formation of a side product, a few red crystals of which separated first on crystallisation from dimethyl sulfoxide. An X-ray diffraction study (see Supporting Information) showed that this minor species has the composition [$Ru^{III}Cl_2(L^2)PPh_3$] (**3**). Repeated crystallisation of **2** from dimethyl sulfoxide did not produce any significant amounts of **3**, thereby preventing its full characterisation. The complex *trans*-[$Ru^{II}Cl(L^1)(HPTA)_2$]Cl_2 (**4**) was prepared by the reaction of 2-acetylpyridine N^4,N^4-dimethylthiosemicarbazone and PTA with [$Ru^{II}Cl_2(dmso)_4$] in absolute ethanol (Figure 1). Complex **4** appears to be the first reported ruthenium(II) complex that contains a thiosemicarbazone and 1,3,5-triaza-7-phosphaadamantane (PTA) as ligands. Complexes **1** and **2** are well soluble in $CHCl_3$ but sparingly soluble in ethanol and methanol and insoluble in water, whereas complex **4** is very soluble in water ($S_{25°C} \geq 250$ mg/mL), dmso, ethanol and methanol.

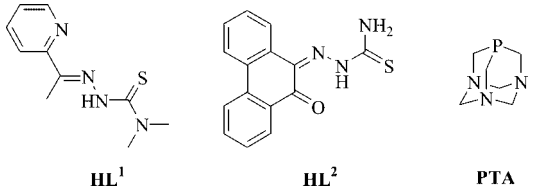

Figure 1. Structures of the ligands used.

Spectroscopic Characterisation

Complexes **1** and **4** show two well-resolved MLCT transitions in their electronic absorption spectra. The bands at 476 (**1**) and 450 nm (**4**) can be attributed to an Ru(4dπ)→π*(py) MLCT transition, whereas the bands at 379 (**1**) and 378 nm (**4**) can be assigned to an Ru(4dπ)→π*(imine) transition.[25] The strong absorptions at 597 and 470 nm in complex **2** are assignable to a combination of MLCT bands and Ru^{II} d–d bands, and the high-energy absorptions in the ultraviolet region for **1**, **2** and **4** can be attributed to intraligand π–π* transitions.

The ESI mass spectrum of complex **1** recorded in the positive mode contains a strong peak at *m*/*z* = 847 attributed to the $[M - Cl]^+$ ion and a second remarkable signal at *m*/*z* = 585 assigned to $[M - Cl - PPh_3]^+$. Complex **2** shows a low intensity peak at *m*/*z* = 942 due to the $[M + H]^+$ ion and more intense peaks at *m*/*z* = 964 and 980 attributed to $[M + Na]^+$ and $[M + K]^+$ ions, respectively. An intense signal at *m*/*z* = 906 corresponds to $[M - Cl]^+$, while that at *m*/*z* = 644 corresponds to $[M - Cl - PPh_3]^+$. The ESI mass spectrum of complex **4** contains peaks at *m*/*z* = 673 and 695, which were assigned to $[M - H]^+$ and $[M - 2H + Na]^+$, respectively. A signal at *m*/*z* = 637 is due to $[M - Cl]^+$, while that at *m*/*z* = 538 is due to $[M - H - HPTA + Na]^+$. The observed isotopic patterns fit well with the theoretical isotopic distributions.

The ^1H NMR spectrum of complex **1** in $CDCl_3$ shows signals attributable to the pyridine ring protons of coordinated thiosemicarbazone at δ = 8.62, 7.36, 6.86 and 6.47 ppm. The lack of any NH signal indicates the deprotonation of the ligand. Proton resonances due to the PPh_3 ligand are found between δ = 7.54 and 7.14 ppm. The ^{31}P NMR spectrum shows one resonance at δ = 30.42 ppm, thus indicating the equivalence of the two PPh_3 ligands in **1**. This signal is shifted only slightly downfield from that for *trans*-[RuCl(pabh)$(PPh_3)_2$] (Hpabh is a Schiff base derived from 2-pyridinecarbaldehyde and benzoylhydrazine) at δ = 27.62 ppm ($CDCl_3$).[31] Complex **2** in [D_6]dmso shows aromatic proton signals for the phenanthrenequinone moiety between δ = 7.19 and 8.89 ppm. The signal integrations and multiplicities are in agreement with the proposed formula, although exact assignment is not possible due to extensive overlap with resonances originating from the triphenylphosphane ligands. A singlet that can be assigned to

the NH_2 group was found at δ = 8.13 ppm. The hydrazinic NNH proton signal at δ = 14.42 ppm present in the ^1H NMR spectrum of the metal-free thiosemicarbazone is absent in the spectrum of the complex, thus indicating the deprotonation of the thiosemicarbazone ligand upon complexation. As for **1**, the ^{31}P NMR spectrum of **2** is very simple, displaying one resonance at δ = 27.36 ppm due to the equivalence of the two PPh_3 ligands.

Complex **4** in [D_6]dmso shows a signal at δ = 9.87 ppm that can be assigned to the protons of the two quaternary nitrogen atoms in the PTA ligands. As for **1**, the absence of a further NH resonance indicates the presence of a monoanionic thiosemicarbazone ligand in **4**. The pyridine ring protons occur as multiplets at δ = 8.77, 7.85, 7.67 and 7.33 ppm. The singlet due to the $N(CH_3)_2$ group is found at δ = 3.33 ppm together with the water signal. The proton resonances of the methylene groups bridging the nitrogen atoms in PTA appear as a singlet at δ = 4.62 ppm, while the resonances due to the PCH_2N protons are observed as a multiplet at δ = 3.71 ppm. The ^{31}P NMR spectrum of **4** exhibits one singlet resonance at δ = –38.13 ppm for the two equivalent PTA ligands {cf. δ = –33.45 ppm for the two equivalent phosphorus atoms in $[RuCl(PTA)_2([9]aneS_3)]$-CF_3SO_3}.[29e]

The electrochemical properties of complexes **1**, **2** and **4** have been studied by cyclic voltammetry in dmso solution (0.2 M [nBu$_4$N][BF_4]) using a glassy carbon working electrode. The cyclic voltammograms of all complexes show a single one-electron oxidation wave at $E_{1/2}$ = 0.59, 0.71 and 0.73 V vs. NHE for **1**, **2** and **4**, respectively, which can be assigned to Ru^{II}/Ru^{III} electron transfer. The peak-to-peak separation (ΔE_p) of 70–90 mV in complexes **1** and **2** is almost independent of the scan rate. In addition, the equality of the anodic peak current (i_{pa}) and the cathodic peak current (i_{pc}) indicates a reversible electron-transfer. The Ru^{II}/Ru^{III} oxidation wave in complex **4** shows ΔE_p values of 110–130 mV in the range of scan rates from 50 to 1000 mV s^{-1} and i_{pa}/i_{pc} ratios close to 1. Deviations from the ideal Nernstian value of 59 mV are well documented for this type of complexes.[26] Complex **2** shows two additional irreversible reduction waves with $E_{p/2}$ values of –0.78 and –1.27 V which can be ascribed to the reduction of the thiosemicarbazone ligand. The more positive oxidation response (+140 mV) in **4** in comparison to that in **1** is in line with the poorer electron-donating ability of PTA compared to PPh_3.[32]

Crystal Structures

The thiosemicarbazone ligand in **1** acts as a monoanion $(L^1)^-$ and occupies a meridional plane about the ruthenium ion, coordinating to it through pyridine nitrogen atom N1, imine nitrogen atom N2 and the thiolate sulfur atom S (Figure 2). A Cl ligand completes the square plane around the ruthenium ion. The thiosemicarbazone ligand is planar. All non-hydrogen atoms of $(L^1)^-$ lie in the crystallographic symmetry plane together with the central metal ion and the chlorido ligand. Two *trans*-positioned triphenylphosphane ligands in **1** complete the octahedron. A comparison of the bond lengths in the coordination polyhedron of **1** with those in $[Ru(HL)(PPh_3)_2Cl]^+$ [HL = 2-acetylpyridine 4-(4-tolyl)thiosemicarbazone][26] shows that the Ru–Cl bond in **1** [2.4812(13) Å] is significantly longer than in $[Ru(HL)(PPh_3)_2Cl]^+$ [2.459(2) Å]. The interatomic Ru–N1 and Ru–N2 distances of 2.092(4) and 1.976(4) Å, respectively, are similar to those in $[Ru(HL)(PPh_3)_2Cl]^+$ [2.085(5) and 1.984(5) Å, respectively], whereas the Ru–S and Ru–P bonds are shorter in **1** {2.3725(13) and 2.3747(8) Å compared to 2.386(2) and 2.399(1) Å in $[Ru(HL)(PPh_3)_2Cl]^+$}. The distribution of electron density over the thiosemicarbazide moiety in the compared complexes is different, thereby indicating the prevailing double-bond character of C8–S in $[Ru(HL)(PPh_3)_2Cl]^+$ [1.707(6) Å vs. 1.751(5) Å in **1**]. The N3–C8 bond length in **1** [1.335(7) Å] is equal within 3σ to that in $[Ru(HL)(PPh_3)_2Cl]^+$ [1.359(7) Å]. The molecules of **1** interact weakly with each other through C–H···Cl contacts, as shown in Figure S1 (Supporting Information).

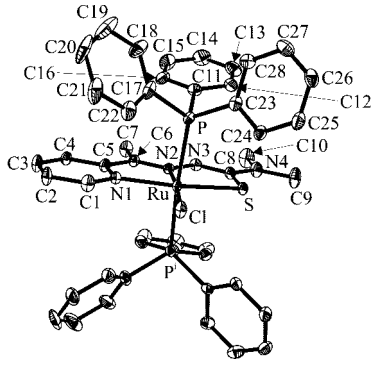

Figure 2. Perspective view of the molecule of $[Ru^{II}(L^1)(PPh_3)_2Cl]$ (**1**) with atom labelling scheme. Thermal ellipsoids are drawn at the 50% probability level, and the hydrogen atoms have been omitted for clarity. Selected bond lengths [Å] and angles [°]: Ru–N1 2.092(4), Ru–N2 1.976(4), Ru–S 2.3725(13), Ru–Cl 2.4812(13), Ru–P1 2.3747(8), S–C8 1.751(5), C8–N3 1.335(7) Å; P1–Ru–P1^i 175.08(6). Symmetry code: ^{i}: $-x$, y + 1, z.

The ruthenium(II) ion in **2** is coordinated by the thiosemicarbazone anion $(L^2)^-$ through carbonyl oxygen atom O, imine nitrogen atom N1 and thiolate sulfur atom S and by the chlorido ligand in the equatorial plane. In addition, two triphenylphosphane ligands are bound in axial positions (Figure 3). Relevant bond lengths and angles are given in the legend to Figure 3. A comparison of the bond lengths of the thiosemicarbazone moiety in complex **2** with those of the metal-free thiosemicarbazone[24] shows that the S–C15 bond [1.707(4) Å] in **2** is longer than in $HL^2{\cdot}CH_3CN$ [1.681(2) Å], whereas the C15–N2 bond [1.348(9) Å] in **2** is similar to that in $HL^2{\cdot}CH_3CN$ [1.365(3) Å]. The coordination of HL^1 and HL^2 (Figure 1) to the ruthenium(II) ion in their deprotonated forms in **1** and **2**, respectively, is also indicated by the absence of counterions. The ligand in **2** has also undergone a configurational change from the (*E*) configuration found in the metal-free state[24] to a (*Z*) configuration relative to the C15–N2 bond. The phenanthrene

moieties in the crystal structure of **2** are stacked pairwise in an offset manner with an interplanar separation between the benzene rings (C9–C14) and (C9–C14)′ of around 3.32 Å; the distance between their centroids (X···X′) is 3.857 Å (Figure S2). The hydrogen bond between N3 as proton donor and the Cl atom of the neighbouring molecule as proton acceptor, with an N3···Cl contact of 3.490 Å, is also worthy of note.

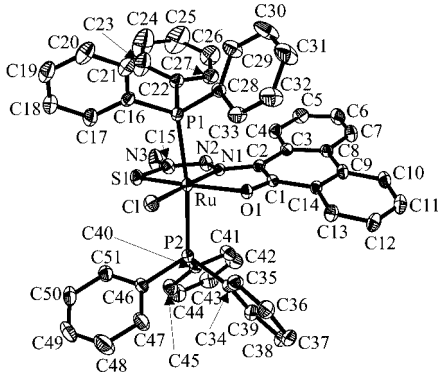

Figure 3. Perspective view of the molecule of $[Ru^{II}(L^2)(PPh_3)Cl]$ (**2**) with atom numbering scheme. Thermal ellipsoids are drawn at the 30% probability level, and the hydrogen atoms have been omitted for clarity. Selected bond lengths [Å] and angles [°]: Ru–O 2.096(2), Ru–N1 1.936(3), Ru–S 2.3608(14), Ru–P1 2.3932(10), Ru–P2 2.3824(10), Ru–Cl 2.4528(9), S–C15 1.707(4), C15–N2 1.348(9) Å; P1–Ru1–P2 170.36(3), O–Ru–S 160.96(6), N1–Ru–Cl 171.31(8).

The structure of complex **4** is shown in Figure 4. The coordination polyhedron of the ruthenium ion can be described as a distorted octahedron. As in **1**, the metal ion is coordinated in the equatorial plane by the thiosemicarbazone monoanion through pyridine nitrogen atom N1, imine nitrogen atom N2 and the thiolate sulfur atom S, and by the chlorido ligand Cl1. Both axial positions are occupied by two PTA ligands, which are bound to the ruthenium ion through phosphorus atoms P1 and P2. The Ru–$P_{(PTA)}$ separations [Ru–P1 2.3019(19), Ru–P2 2.2958(19) Å] are in the range expected for Ru–PTA complexes.[30,33] The Ru–Cl1 bond [2.4571(16) Å] is normal for Ru–PTA complexes containing chlorido co-ligands.[34] In addition, the two PTA ligands are protonated at N5 and N8, respectively, and form hydrogen bonds to Cl2 and Cl3. The S–C8 bond [1.771(6) Å] is longer than the C–S bond found in 2-acetylpyridine *N*-pyrrolidinylthiosemicarbazone [1.692(4) Å][35] and also longer than in HL^1 [1.720(2) Å].[36] The lengthening of this bond in **4**, along with the N2–N3 and N3–C8 bonds, indicates a significant electron delocalisation over the thiosemicarbazide moiety.[37] The Ru–N2 distance [1.979(5) Å] is slightly shorter than the Ru–N1 distance [2.081(5) Å], presumably because of steric reasons. The association of a proton with N5 of one PTA and of another one with N8 of the second PTA ligand makes the corresponding atoms good proton donors, and they are consequently involved in hydrogen bonding to the two chloride anions Cl2 and Cl3, respectively (see Figure 4).

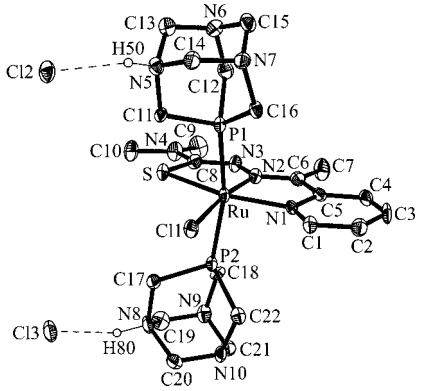

Figure 4. Perspective view of the complex $[Ru^{II}(L^1)(HPTA)_2Cl]Cl_2$ (**4**) with atom numbering scheme. Thermal ellipsoids are drawn at the 50% probability level, and the hydrogen atoms have been omitted for clarity. Selected bond lengths [Å] and angles [°]: Ru–N1 2.081(5), Ru–N2 1.979(5), Ru–S 2.3707(17), Ru–Cl1 2.4571(16), Ru–P1 2.3019(19), Ru–P2 2.2958(19), S–C8 1.771(6), C8–N3 1.303(8); P1–Ru–P2 166.05(5).

Determination of the pK_a Value

The pH of a 0.005 M aqueous solution of $[Ru^{II}Cl(L^1)(HPTA)_2]Cl_2$ (**4**) is about 3. ^{31}P NMR spectra of an aqueous (D_2O) solution of **4** were recorded at different pH* (= pD) values (from 2.11 to 11.40). We suppose that the complex exists predominantly in the monoprotonated form (δ = –37.03 ppm) at pH* = 2.11, whereas the signal of the neutral complex (with unprotonated PTA ligands) is found at δ = –48.45 ppm at pH* = 11.40 (see Figure S4, Supporting Information). At pH = 3.82 the main signal is shifted to δ = –40.02 ppm and a second, minor (< 4%) ^{31}P signal emerges at δ = –41.30 ppm, which increases gradually in intensity and shifts to higher frequency more sluggishly than the first peak (Figure S4). At the end of the titration (pH* = 11.40) the intensity of the second signal is 50% of the main signal. Moreover, the intensity of this second resonance increases with time. The appearance of this second ^{31}P resonance can be suppressed by addition of an excess of NaCl to a solution of **4** in D_2O. Repeated titration of a 0.15 M NaCl solution of **4** in D_2O with NaOD from pH* = 3.29 to 10.30 showed that the second peak now appears first at pH = 5.16 and remains of very low intensity (< 5%) until the end of the titration (pH = 10.30). These results show that a solution of complex **4** in D_2O in the pH range indicated above undergoes both protolytic reactions and hydrolysis of the Ru^{II}–Cl bond.

A pK_a value of 4.46 for one of the axially coordinated PTA ligands in **4** was obtained from a ^{31}P NMR pH* titration curve in D_2O (Figure 5). This value is higher than that (3.13) found from ^{31}P NMR titration of the coordinated PTA in $[RuCl_2(PTA)(\eta^6\text{-}p\text{-cymene})]$,[38] but lower than those reported for metal-free PTA (5.63[29c] and 6.0[39]).

The evolution of the absorption spectrum of **4** in 0.15 M NaCl aqueous solution on increasing the pH from 2.88 to 9.30 is given as Supporting Information (Figure S5) and is characterised by an isosbestic point at 445 nm.

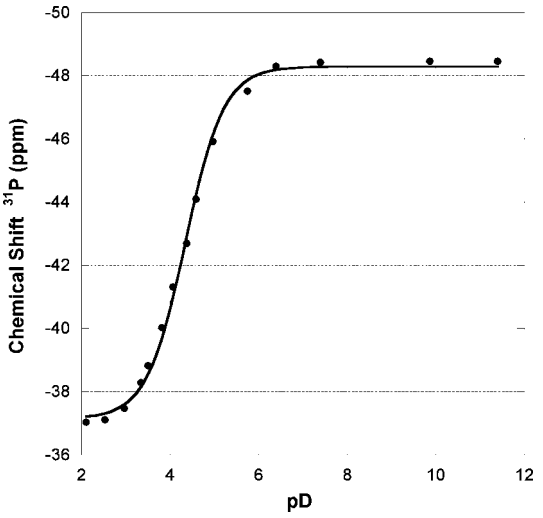

Figure 5. Plot of $\delta(^{31}P)$ vs. pD of **4**.

Antiproliferative Activity in Cancer Cell Lines

The antiproliferative effects of compound **4** were first examined in the human cancer cell lines 41M and SK-BR-3 by means of a colourimetric microculture assay (MTT assay) with continuous exposure at pH = 7.4 for 96 h. Concentration-effect curves are presented in Figure 6A. The compound exerts strong antiproliferative effects in low micromolar concentrations in the ovarian carcinoma cell line 41M (IC_{50} = 0.87 μM), while the breast cancer cell line SK-BR-3 is much less sensitive (IC_{50} = 39 μM). The IC_{50} values obtained in the non-small cell lung cancer cell line A549 and the colon carcinoma cell line HT-29 (Table 1) suggest that these cells are rather insensitive, but a direct comparison with the other two cell lines is not appropriate because of the different exposure times. However, experiments on the pH dependency of the antiproliferative effects, with exposure at either pH = 6.0 or 7.4 for 24 h, followed by incubation in a drug-free medium (pH = 7.4) for a further 72 h revealed that the activity of the compound is 6.5- and 5.4-times higher under slightly acidic conditions in A549 and HT-29 cells, respectively, with IC_{50} values shifted towards lower micromolar concentrations (Figure 6B, Table 1). The extent of this activation clearly exceeds that of cisplatin (3.2- and 2.2-fold in A549 and HT-29 cells, respectively), while the effects of oxaliplatin are independent of the pH under the same experimental conditions.[40]

This pronounced pH dependency suggests that compound **4** may be activated preferentially in a slightly acidic environment. Such acidic conditions occur in the extracellular fluid of solid tumours as a consequence of constitutive upregulation of glycolysis (independent of oxygen supply), which is a hallmark of malignant progression that confers a growth advantage to tumour cells under the conditions of intermittent hypoxia resulting from hypovascularisation.[41,42] The altered pH gradients across cell membranes in acidic tumour regions affect the cellular drug accumulation and cytotoxicity of weakly basic chemotherapeutics such as anthracyclines, vinca alkaloids or mitoxantrone and

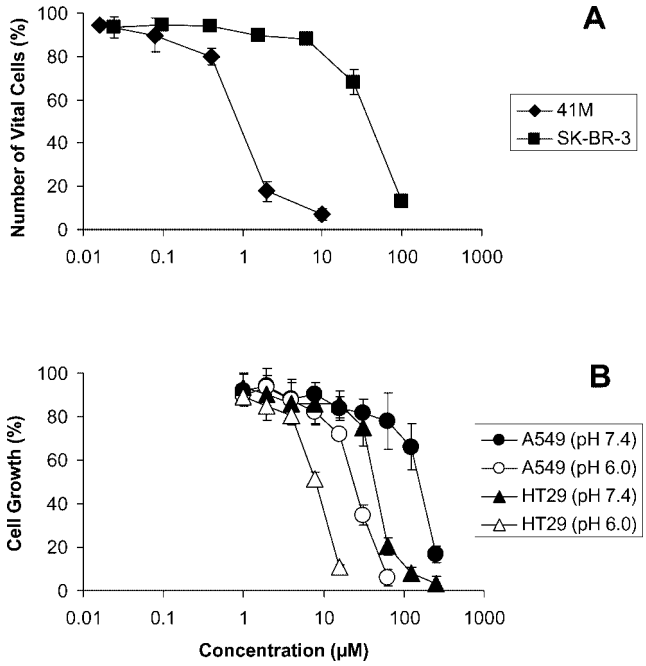

Figure 6. Antiproliferative effects of compound **4**, as determined by an MTT assay. A) Concentration-effect curves in 41M and SK-BR-3 cells (continuous exposure for 96 h). B) Concentration-effect curves (corrected for differences in growth kinetics of the corresponding controls) in A549 and HT-29 cells at pH = 7.4 and 6.0 (24 h exposure), indicating enhanced cytostatic effects in a slightly acidic medium.

Table 1. Antiproliferative effects of compound **4** in four human cancer cell lines and the pH dependency in two of these cell lines.

Cell line	Exposure time [h]	IC_{50} [μM][a] pH = 7.4	GI_{50} [μM][b] pH = 7.4	pH = 6.0	GI_{50} ratio
41M (ovary)	96	0.87±0.09			
SK-BR-3 (breast)	96	39±5			
A549 (lung)	24	186±16	156±18	24±1	6.5
HT29 (colon)	24	47±4	43±4	8.0±0.4	5.4

[a] 50% inhibitory concentrations in the MTT assay. [b] 50% growth inhibition (corrected for differences in growth kinetics of the corresponding controls) after exposure for 24 h in the MTT assay. All values are the means with standard deviations obtained from at least three independent experiments.

may therefore contribute to the reduced chemosensitivity of acidic tumours.[43–45] On the other hand, weakly acidic drugs such as chlorambucil are more cytotoxic when the extracellular pH is slightly acidic.[44,46] These observations are consistent with ion trapping, according to which weak electrolytes that are not transported actively concentrate in the compartment where their ionised fraction is larger. Ion trapping has also been discussed as a possible explanation for the pH-dependent cellular uptake and cytotoxicity of the metal complex cisplatin, the hydrolysis products of which are in a pH-dependent equilibrium.[47] Therefore, the importance of appropriate pK_a values for the design of antitumour drugs has been emphasised.[48] Furthermore, the development of prodrugs that are selectively activated in an acidic environment is being pursued as a strategy to in-

crease the therapeutic index by effectively killing tumour cells without impairing normal tissues.[49]

Some (PTA)ruthenium(II) complexes related to the compounds presented here have been found to induce DNA damage in isolated bacterial plasmids only at pH values less than about 7.0[50] and to exert a stronger cytotoxicity in breast cancer cells than in a non-malignant mammary gland cell line, while analogues containing methylated PTA, which is not protonated in acidic solution, do not show this kind of selectivity.[38] PTA has therefore attracted attention as a ligand that apparently confers tumour selectivity to (arene)ruthenium(II) compounds, which has been tentatively attributed to activation by protonation (assuming that the protonated form is actually the active species). While it has not been reported whether the cytotoxicity of arene–Ru^{II}–PTA complexes is pH-dependent, our findings with compound **4**, which exerts stronger antiproliferative effects at pH values encountered in solid tumours (6.0) than at pH values prevailing in normal tissues (7.4), support this notion. The presence of two PTA ligands in compound **4** may be favourable from this point of view and may constitute a basis for further attempts to increase tumour-selective activity. However, the pronounced decrease of pK_a (from 5.6 to 3.0–3.3) resulting from the coordination of PTA to ruthenium(II) in arene–Ru^{II}–PTA complexes renders the possibility that ion trapping accounts for any pH-dependent cytotoxicity of this type of compounds rather unlikely[38] and raises the need for other explanations that might be completely different from previous assumptions.

In contrast to arene–Ru^{II}–PTA complexes, the presence of the biologically active thiosemicarbazone ligand may play a role in the activity of complex **4** even though this ligand is tightly bound to the metal centre in a tridentate manner. However, even a partial release of 2-acetylpyridine N^4,N^4-dimethylthiosemicarbazone should result in a tremendous increase in cytotoxicity because its IC_{50} values of 0.22 and 2.7 nM in 41M and SK-BR-3 cells, respectively,[23] are three to four orders of magnitude below those of complex **4**. If a release of the thiosemicarbazone ligand accounts for the effects of compound **4**, it must be assumed to occur only to a very small degree.

Conclusions

Following a known approach based on using P-containing derivatives as co-ligands, a novel highly water-soluble ruthenium(II) thiosemicarbazonate complex, namely $[Ru^{II}(L^1)(HPTA)_2Cl]Cl_2$, has been prepared. This, to the best of our knowledge, is the first ruthenium(II) complex with mixed thiosemicarbazone/PTA ligands to be isolated and characterised by X-ray crystallography. The complex shows pH-dependent antiproliferative activity in vitro in micromolar concentrations against the non-small cell lung cancer cell line A549 and the colon carcinoma cell line HT29.

Experimental Section

General: All chemicals were obtained from commercial suppliers and were used without further purification. Phenanthrenequinone thiosemicarbazone,[24] 2-acetylpyridine N^4,N^4-dimethylthiosemicarbazone,[51] 1,3,5-triaza-7-phosphaadamantane (PTA)[52] and *cis*-$[RuCl_2(dmso)_4]$[53] were prepared according to published procedures. Elemental analyses were carried out at the Institute of Physical Chemistry of the University of Vienna with a Carlo Erba microanalyser. Infrared spectra were recorded with a Bruker Vertex 70 FTIR spectrometer as KBr pellets (4000–400 cm^{-1}). Electronic spectra were obtained with a Perkin–Elmer Lambda 650 UV/Vis spectrophotometer. Electrospray ionisation mass spectrometry was carried out in methanol with a Bruker Esquire 3000 instrument (Bruker Daltonics, Bremen, Germany). Expected and experimental isotope distributions were compared. The NMR spectra were recorded with a Bruker DPX 400 instrument using standard Bruker pulse programs. Chemical shifts for ^1H NMR spectra were referenced to the residual ^1H present in deuterated dmso and $CHCl_3$, respectively, and ^{31}P NMR to external $H_3{}^{31}PO_4$ in D_2O. Cyclic voltammograms were measured in a three-electrode cell using a 0.2-mm-diameter glassy carbon working electrode, a platinum auxiliary electrode and an $Ag|Ag^+$ reference electrode containing 0.1 M $AgNO_3$, the potential of which was corrected using an internal standard redox couple of ferrocenium/ferrocene. Measurements were performed at room temperature using an EG & G PARC 273A potentiostat/galvanostat. Deaeration of solutions was accomplished by passing a stream of argon through the solution for 5 min prior to the measurements and then maintaining a blanket of argon over the solution during the measurement. The potentials were measured in 0.2 M $[nBu_4N][BF_4]$/dmso, with $[Fe(\eta^5\text{-}C_2H_5)_2]$ ($E_{1/2}{}^{ox}$ = +0.68 V vs. NHE)[54] as internal standard, and are quoted relative to NHE.

$[RuL^1Cl(PPh_3)_2]$ (1): A suspension of 2-acetylpyridine N^4,N^4-dimethylthiosemicarbazone (22.3 mg, 0.1 mmol) in dry dichloromethane (5 mL) was added to a solution of $[RuCl_2(PPh_3)_3]$ (95.8 mg, 0.1 mmol) in dry dichloromethane (5 mL) and the resulting mixture was refluxed under argon for 4 h. The solution was concentrated to about 5 mL, and allowed to stand at +4 °C overnight. The product was obtained as green-brown crystals, which were filtered off, washed with *n*-hexane and dried in vacuo. Yield: 36 mg (41%). $C_{46}H_{43}ClN_4P_2RuS\cdot0.5CH_2Cl_2$ (924.86): calcd. C 60.39, H 4.80, N 6.06, S 3.47; found C 60.61, H 4.80, N 6.30, S 3.57. ESI-MS: *m*/*z* = 847 $[M - Cl^-]^+$, 585 $[M - Cl^- - PPh_3]^+$. IR: $\tilde{\nu}$ = 1522 [w, $\nu_{(C=N)}$], 1482 (m), 1391 (s), 1314 (s), 907 (w), 742 (m), 695 (s) and 516 (s, $\nu_{[Ru(PPh_3)_2]}$) cm^{-1}. ^1H NMR (400.13 MHz. $CDCl_3$): δ = 8.62 (d, $^3J_{H,H}$ = 5.1 Hz, 1 H, py), 7.54–7.51 (m, 12 H, PPh_3), 7.36 (m, 1 H, py), 7.24–7.21 (m, 6 H, PPh_3), 7.18–7.14 (m, 12 H, PPh_3), 6.86 (d, $^3J_{H,H}$ = 8.1 Hz, 1 H, py), 6.47 (t, $^3J_{H,H}$ = 6.2 Hz, 1 H, py), 2.70 [s, 6 H, $N(CH_3)_2$], 1.82 [s, 3 H, $C(CH_3)$] ppm. $^{31}P\{^1H\}$ (162.00 MHz; $CHCl_3$): δ = 30.42 and 26.19 [equal intensity $(PPh_3)_2$] ppm. UV/Vis (CH_2Cl_2): λ_{max} (ε) = 599 sh (1620), 546 sh (2280), 476 (7500), 397 sh (31760), 379 (39880), 274 (47120 $M^{-1}cm^{-1}$) nm. Single crystals suitable for an X-ray diffraction study were selected directly from the reaction vessel.

$[RuL^2Cl(PPh_3)_2]\cdot C_2H_5OH$ (2). Method a): A suspension of phenanthrenequinone thiosemicarbazone (28.2 mg, 0.1 mmol) in dry ethanol (5 mL) was added to a suspension of $[RuCl_2(PPh_3)_3]$ (95.8 mg, 0.1 mmol) in dry ethanol (5 mL), and the resulting mixture was refluxed under argon for 4 h. The solution was concentrated to about 5 mL and allowed to stand at +4 °C overnight. The solid residue was stirred in *n*-hexane to remove the excess of ligand and triphenylphosphane, filtered off and dried in vacuo. Yield: 61 mg (65%). $C_{51}H_{40}ClN_3OP_2RuS\cdot C_2H_5OH$ (987.49): calcd. C 64.46, H 4.70, N 4.26, S 3.25; found C 64.46, H 4.36, N 4.55, S 3.34. ESI-MS: *m*/*z* = 942 $[M + H^+]^+$, 964 $[M + Na^+]^+$, 980 $[M + K^+]^+$, 906 $[M - Cl^-]^+$, 644 $[M - Cl^- - PPh_3]^+$. IR: $\tilde{\nu}$ = 1600 [s, $\nu_{(C=N)}$], 1590

(s), 1434 (s), 1190 (s), 743 (m), 694 (s) and 519 (s, $\nu_{[Ru(PPh_3)_2]}$) cm^{-1}. ^1H NMR (400.13 MHz, [D$_6$]dmso): δ = 8.88 (dd, $^3J_{H,H}$ = 8.3, $^4J_{H,H}$ = 1.8 Hz, 1 H, phq), 8.43 (dd, $^3J_{H,H}$ = 7.8, $^4J_{H,H}$ = 1.0 Hz, 1 H, phq), 8.35 (d, $^3J_{H,H}$ = 8.6 Hz, 1 H, phq), 8.26 (m, 1 H, phq), 8.13 (s, 2 H, NH_2), 7.65 (m, 1 H, phq), 7.52–7.49 (m, 12 H, PPh_3), 7.26–7.19 (m, 9 H, PPh_3 and phq), 7.14–7.11 (m, 12 H, PPh_3) ppm. $^{31}P\{^1H\}$ (162.00 MHz, [D$_6$]dmso): δ = 27.36 [s, 2 P, $(PPh_3)_2$]. UV/Vis (CH_2Cl_2): λ_{max} (ε) = 597 nm (9080) , 470 (14580), 320 (13600), 268 (49330 $M^{-1}cm^{-1}$) nm. **Method b). [RuL^{2}Cl(PPh$_3$)$_2$]:** Phenanthrenequinone thiosemicarbazone (28.2 mg, 0.1 mmol) in dry ethanol (5 mL) and triphenylphosphane 76.0 mg (0.29 mmol) in dry ethanol (5 mL) were added to [$RuCl_2$(dmso)$_4$] (48.0 mg, 0.1 mmol) in dry ethanol (5 mL) and the mixture refluxed under argon for 5 h. The black solid was filtered off, washed with absolute ethanol and *n*-hexane and dried in vacuo. Yield: 79 mg (80%). $C_{51}H_{40}ClN_3OP_2RuS$ (941.42): calcd. C 65.07, H 4.28, N 4.46; found C 64.78, H 4.43, N 4.38. Single crystals suitable for X-ray data collection were obtained from a chloroform solution of **2** saturated with *n*-hexane.

[RuL^{1}Cl(HPTA)$_2$]Cl$_2$·C$_2$H$_5$OH·H$_2$O (4·C$_2$H$_5$OH·H$_2$O): A solution of 2-acetylpyridine N^4,N^4-dimethylthiosemicarbazone (22.3 mg, 0.1 mmol) in dry ethanol (5 mL) was added to a suspension of *cis*-[$RuCl_2$(dmso)$_4$] (44.8 mg, 0.1 mmol) in dry ethanol (5 mL), and the resulting mixture was heated at 65 °C under argon for 1 h to yield a red solution. PTA (31.6 mg, 0.2 mmol) was then added and heating was continued for a further 4 h. The green-yellow side product was separated by filtration and the red solution concentrated to about 1 mL and allowed to stand at +4 °C overnight. The red crystals formed were filtered off, washed with cold dry ethanol and dried in vacuo. Yield: 7 mg (10%). $C_{22}H_{39}Cl_3N_{10}P_2RuS{\cdot}C_2H_5OH{\cdot}H_2O$ (809.14): calcd. C 35.63, H 5.85, N 17.31, S 3.96; found C 35.09, H 5.40, N 17.49, S 4.07. ESI-MS: *m*/*z* = 673 [M – H^+]$^+$, 695 [M – 2 H^+ + Na^+]$^+$, 637 [M – 2 H^+ – Cl^-]$^+$, 538 [M – 2 H^+ – PTA + Na^+]$^+$. IR: $\tilde{\nu}$ = 1531 [w, $\nu_{(C=N)}$], 1503 (w), 1397 (s), 1315 (s), 768 (m), 566 (m) cm^{-1}. ^1H NMR (400.13 MHz, [D$_6$]dmso): δ = 9.87 (s, 2 H, NH), 8.77 (d, $^3J_{H,H}$ = 5.3 Hz, 1 H, py), 7.85 (m, 1 H, py), 7.67 (d, $^3J_{H,H}$ = 8.1 Hz, 1 H, py), 7.33 (m, 1 H, py), 4.62 (s, 12 H, NCH_2N), 3.78–3.67 (m, $^3J_{H,P}$ = 10.6 Hz, 12 H, NCH_2P), 3.33 [s, 6 H, $N(CH_3)_3$, below the water signal], 2.42 (s, 3 H, CH_3) ppm. $^{31}P\{^1H\}$ (162.00 MHz, [D$_6$]dmso): δ = –38.13 [s, 2 P, $(HPTA)_2$]. UV/Vis (H_2O): λ_{max} (ε) = 522 sh (870), 450 (5460), 378 sh (18320), 355 (25910), 280 sh (9220), 222 sh (38930 $M^{-1}cm^{-1}$) nm. Red crystals of composition **4**·2H_2O of X-ray diffraction quality were obtained by recrystallisation from ethanol.

Determination of the pK_a Values: The pH* titration experiment was carried out in D_2O at 298 K using an Ecoscan pH 6 (Eutech) pH meter equipped with a micro-combination pH electrode (Orion) for NMR tubes calibrated with buffer solution at pH = 4, 7 and 10. The pH* values were adjusted with diluted DCl and NaOD. The pK_a value of the coordinated PTAs in **4** was determined by plotting the change in chemical shift of the ^{31}P signal against pH* and fitting the curve to the modified Henderson–Hasselbalch equation[55] (δ_{obs}, δ_{HA} and δ_A are the chemical shifts for the observed, protonated and deprotonated species, respectively), by using the program KALEIDAGRAPH,[56] with the assumption that the observed values are weighted averages according to the populations of the protonated and deprotonated species.

$$\delta_{obs} = \frac{\delta_{HA} + \delta_A \cdot 10^{(pH-pK_a)}}{1+10^{(pH-pK_a)}}$$

The pK_a* value determined from the titration curve in Figure 5 was corrected by using the equation pK_a = 0.929 pK_a* + 0.42 suggested by Krezel and Bal,[57] (with pK_a* as the pK_a value determined in D_2O) for conversion of protonation constants, measured in D_2O into constants valid for H_2O solutions. The error is estimated as ±0.04 pK units for two ^{31}P resonances, and the mean value was taken.

X-ray Crystallography: X-ray diffraction measurements were performed with an X8 APEXII CCD diffractometer. Single crystals of **1**–**4** were positioned at 40, 40, 40 and 37.5 mm from the detector, respectively, and 1187, 1438, 1328 and 1320 frames were measured each for 70, 120, 50 and 10 s with a 1° scan-width. The data were processed using the SAINT software package.[58] The structures were solved by direct methods and refined by full-matrix least-squares techniques. Non-hydrogen atoms were refined with anisotropic displacement parameters. H atoms were inserted in geometrically calculated positions and refined with a riding model. The following computer programs were used: structure solution: SHELXS-97;[59] refinement: SHELXL-97;[60] molecular diagrams: ORTEP;[61] computer CPU: Pentium IV; scattering factors were taken from the literature.[62] Crystal data, data collection parameters, and structure refinement details are given in Table 2. CCDC-630689 (**1**·3CH_2Cl_2), -630686 (**2**), -630687 (**3**·dmso·1.25H_2O) and -630688 (**4**·2H_2O) contain the supplementary crystallographic data for this paper. These data can be obtained free of charge from The Cambridge Crystallographic Data Centre via www.ccdc.cam.ac.uk/data_request/cif.

Cell Lines and Culture Conditions: Human 41M (ovarian carcinoma) and SK-BR-3 (mammary carcinoma) cells were kindly provided by Lloyd R. Kelland (CRC Centre for Cancer Therapeutics, Institute of Cancer Research, Sutton, UK) and Evelyn Dittrich (General Hospital, Medical University of Vienna, Austria), respectively. Human A549 (non-small cell lung cancer) and HT29 (colon carcinoma) cells were kindly provided by Brigitte Marian (Institute of Cancer Research, Medical University of Vienna, Austria). Cells were grown in 75-cm^2 culture flasks (Iwaki/Asahi Technoglass, Gyouda, Japan) as adherent monolayer cultures in complete culture medium [Minimal Essential Medium (MEM) supplemented with 10% heat-inactivated fetal bovine serum, 1 mM sodium pyruvate, 4 mM L-glutamine and 1% non-essential amino acids (100×) (all purchased from Sigma–Aldrich, Vienna, Austria)]. Cultures were maintained at 37 °C in a humidified atmosphere containing 5% CO_2.

Antiproliferative Activity in Cancer Cell Lines: Antiproliferative effects were determined by means of a colourimetric microculture assay [MTT assay; MTT = 3-(4,5-dimethyl-2-thiazolyl)-2,5-diphenyl-2*H*-tetrazolium bromide]. Cells were harvested from the culture flasks by trypsinisation and seeded into 96-well microculture plates (Iwaki/Asahi Technoglass, Gyouda, Japan) in cell densities of 4×10^3 (except HT-29: 3×10^3 cells/well), in order to ensure exponential growth throughout drug exposure. After pre-incubation for 24 h, 41M and SK-BR-3 cells were exposed to serial dilutions of the test compound in 200 μL/well complete culture medium for 96 h under an atmosphere containing 5% CO_2. For pH-dependency experiments in A549 and HT-29 cells, the test compound was dissolved in Dulbecco's Modified Eagles Medium (DMEM) (w/o sodium hydrogencarbonate) supplemented with 10% heat-inactivated fetal bovine serum, 1 mM sodium pyruvate, 4 mM L-glutamine, 1% non-essential amino acids (100×) and sodium hydrogencarbonate in either 8.8 mM (pH = 6.0) or 39.6 mM (pH = 7.4) concentration (all purchased from Sigma–Aldrich, Vienna, Austria), and cells were exposed under an atmosphere containing 8% CO_2 for 24 h, followed by incubation in 200 μL/well drug-free DMEM (pH = 7.4) for a further 72 h. At the end of

Table 2. Crystal data and details of data collection for **1**–**4**.

	1·3CH_2Cl_2	**2**	**3**·dmso·1.25H_2O	**4**·2H_2O
Empirical formula	$C_{49}H_{49}Cl_7N_4P_2RuS$	$C_{51}H_{40}ClN_3OP_2RuS$	$C_{35}H_{33.5}Cl_2N_3O_{3.25}PRuS_2$	$C_{22}H_{43}Cl_3N_{10}O_2P_2RuS$
Formula mass	1137.14	941.38	814.70	781.08
Space group	$Pmn2_1$	$P\bar{1}$	$P2_1/c$	$C2/c$
a [Å]	18.4882(7)	9.4527(4)	9.8926(3)	31.404(4)
b [Å]	9.3773(3)	11.8536(7)	17.8078(6)	9.0952(9)
c [Å]	14.7549(6)	20.2796(11)	21.7962(7)	25.571(3)
α [°]		81.177(4)		
β [°]		84.411(3)	95.493(2)	106.939(12)
γ [°]		72.261(3)		
V [Å^3]	2558.05(16)	3822.1(2)	3822.1(2)	6986.8(14)
Z	2	2	4	8
λ [Å]	0.71073	0.71073	0.71073	0.71073
$\rho_{calcd.}$ [g cm^{-3}]	1.476	1.464	1.417	1.485
Crystal size [mm]	0.18 × 0.16 × 0.14	0.16 × 0.07 × 0.05	0.34 × 0.20 × 0.18	0.06 × 0.06 × 0.06
T [K]	100	296	100	100
μ [cm^{-1}]	81.4	59.7	73.9	86.6
Flack parameter	–0.01(3)			
R_1[a]	0.0359	0.0413	0.0539	0.0522
wR_2[b]	0.0891	0.1025	0.1631	0.1388
GOF[c]	1.051	0.997	1.093	1.058

[a] $R_1 = \Sigma||F_o| - |F_c||/\Sigma|F_o|$. [b] $wR_2 = \{\Sigma[w(F_o^2 - F_c^2)^2]/\Sigma[w(F_o^2)^2]\}^{1/2}$. [c] GOF = $\{\Sigma[w(F_o^2 - F_c^2)^2]/(n - p)\}^{1/2}$, where n is the number of reflections and p is the total number of parameters refined.

incubation, all media were replaced by 150 μL/well RPMI 1640 medium (supplemented with 10% heat-inactivated fetal bovine serum and 2 mM L-glutamine) plus 20 μL/well MTT solution in phosphate-buffered saline (5 mg/mL). After incubation for 4 h, the medium/MTT mixtures were removed and the formazan crystals formed by the mitochondrial dehydrogenase activity of vital cells were dissolved in 150 μL of dmso per well. Optical densities at 550 nm were measured with a microplate reader (Tecan Spectra Classic), using a reference wavelength of 690 nm to correct for unspecific absorption. The quantity of vital cells was expressed in terms of T/C values by comparison with untreated control microcultures, and 50% inhibitory concentrations (IC_{50}) were calculated from concentration-effect curves by interpolation. In order to correct for differences in growth kinetics in the pH-dependency experiments, concentration-effect curves were transformed by taking the optical densities of separate MTT-stained control microcultures at the beginning of drug exposure as zero values, and GI_{50} concentrations were calculated instead of IC_{50} values. Evaluation is based on the mean of at least three independent experiments, each comprising at least six microcultures per concentration level.

Supporting Information (see footnote on the first page of this article): Crystal packing of complexes **1** and **2**, the molecular structure of **3**, ^{31}P NMR spectra of **4**, UV/Vis spectra of **4** at different pH values and IR spectra of **1**, **2** and **4**.

Acknowledgments

The authors would like to thank the Austrian Science Fund (FWF), the Austrian Council for Research and Technology Development, the Austrian Research Promotion Agency (FFG), the European Cooperation in the Field of Scientific and Technical Research (COST) and the Faustus Forschung Austria Translational Drug Development AG, Vienna, Austria for financial support. We also thank Dr. Hanspeter Kählig for NMR titrations and Mag. Raffael Schuecker for helpful discussions, as well as Mag. Michael Grössl for ESI-MS measurements.

[1] T. S. Lobana, S. Khanna, R. J. Butcher, A. D. Hunter, M. Zeller, *Polyhedron* **2006**, *25*, 2755–2763.
[2] F. Basuli, M. Ruf, C. G. Pierpont, S. Bhattacharya, *Inorg. Chem.* **1998**, *37*, 6113–6116.
[3] G. Dessy, V. Fares, L. Scaramuzza, A. A. G. Tomlinson, G. De Munno, *J. Chem. Soc., Dalton Trans.* **1978**, 1549–1554.
[4] D. Kovala-Demertzi, P. N. Yadav, J. Wiecek, S. Skoulika, T. Varadinova, M. A. Demertzis, *J. Inorg. Biochem.* **2006**, *100*, 1558–1567.
[5] D. X. West, S. B. Padhye, P. B. Sonawane, *Struct. Bonding* **1991**, *76*, 1–50.
[6] E. C. Moore, A. C. Sartorelli, *Pharm. Ther.* **1984**, *24*, 439–447.
[7] E. C. Moore, A. C. Sartorelli, in *Inhibitors of Ribonucleoside Diphosphate Reductase Activity* (Eds.: J. G. Cory, A. H. Cory), Pergamon Press, Oxford, **1989**, pp. 203–215.
[8] E. C. Moore, A. C. Sartorelli, *Pharm. Ther.* **1984**, *24*, 439–447.
[9] R. W. Brockman, J. R. Thomson, M. J. Bell, H. E. Skipper, *Cancer Res.* **1956**, *16*, 167–170.
[10] L. Feun, M. Modiano, K. Lee, J. Mao, A. Marini, N. Savaraj, P. Plezia, B. Almassian, E. Colacino, J. Fischer, S. MacDonald, *Cancer Chemother. Pharmacol.* **2002**, *50*, 223–229.
[11] J. Murren, M. Modiano, C. Clairmont, P. Lambert, N. Savaraj, T. Doyle, M. Sznol, *Clin. Cancer Res.* **2003**, *9*, 4092–4100.
[12] A. Gómez Quiroga, C. Navarro Raninger, *Coord. Chem. Rev.* **2004**, *248*, 119–133.
[13] N. Farrell, *Coord. Chem. Rev.* **2002**, *232*, 1–4.
[14] U. Abram, K. Ortner, R. Gust, K. Sommer, *J. Chem. Soc., Dalton Trans.* **2000**, 735–744.
[15] M. Belicchi-Ferrari, F. Bisceglie, C. Casoli, S. Durot, I. Morgenstern-Badara, G. Pelosi, E. Pilotti, S. Pinelli, P. Tarasconi, *J. Med. Chem.* **2005**, *48*, 1671–1675.
[16] V. B. Arion, M. A. Jakupec, M. Galanski, P. Unfried, B. K. Keppler, *J. Inorg. Biochem.* **2002**, *91*, 298–305.
[17] J. Patole, S. Padhye, M. S. Moodbidri, N. Shirsat, *Eur. J. Med. Chem.* **2005**, *40*, 1052–1055.
[18] L. Otero, M. Vieites, L. Boiani, A. Denicola, C. Rigol, L. Opazo, C. Olea-Azar, J. D. Maya, A. Morello, L. Krauth-Siegel, O. E. Piro, E. Castellano, M. González, D. Gambino, H. Cerecetto, *J. Med. Chem.* **2006**, *49*, 3322–3331.

[19] U. K. Mazumder, M. Gupta, S. S. Karki, S. Bhattacharya, S. Rathinasamy, S. Thangavel, *Chem. Pharm. Bull.* **2004**, *52*, 178–185.
[20] F. Bregant, S. Pacor, S. Ghosh, S. K. Chattopadhyah, G. Sava, *Anticancer Res.* **1993**, *13*, 1011–1017.
[21] G. Sava, R. Gagliardi, A. Bergamo, E. Alessio, G. Mestroni, *Anticancer Res.* **1999**, *19*, 969–972.
[22] M. Galanski, V. B. Arion, M. A. Jakupec, B. K. Keppler, *Curr. Pharm. Des.* **2003**, *9*, 2078–2089.
[23] C. R. Kowol, R. Berger, R. Eichinger, A. Roller, M. A. Jakupec, P. P. Schmidt, V. B. Arion, B. K. Keppler, *J. Med. Chem.* **2007**, *50*, 1254–1265.
[24] Z. Afrasiabi, E. Sinn, S. Padhye, S. Dutta, S. Padhye, C. Newton, C. E. Anson, A. K. Powell, *J. Inorg. Biochem.* **2003**, *95*, 306–314.
[25] M. Maji, S. Ghosh, S. K. Chattopadhyay, T. C. W. Mak, *Inorg. Chem.* **1997**, *36*, 2938–2943.
[26] M. Maji, M. Chatterjee, S. Ghosh, S. Kumar Chattopadhyay, B. M. Wu, T. C. W. Mak, *J. Chem. Soc., Dalton Trans.* **1999**, 135–140.
[27] F. Basuli, S. M. Peng, S. Bhattacharya, *Inorg. Chem.* **2000**, *39*, 1120–1127.
[28] F. Basuli, S. M. Peng, S. Bhattacharya, *Inorg. Chem.* **2001**, *40*, 1126–1133.
[29] a) W. H. Ang, P. J. Dyson, *Eur. J. Inorg. Chem.* **2006**, 4003–4018; b) A. D. Phillips, L. Gonsalvi, A. Romerosa, F. Vizza, M. Peruzzini, *Coord. Chem. Rev.* **2004**, *248*, 955–993; c) W. H. Ang, E. Daldini, C. Scolaro, R. Scopelliti, L. Juillerat-Jeannerat, P. J. Dyson, *Inorg. Chem.* **2006**, *45*, 9006–9013; d) C. Scolaro, T. J. Geldbach, S. Rochat, A. Dorcier, C. Gossens, A. Bergamo, M. Cocchietto, I. Tavernelli, G. Sava, U. Rothlisberger, P. J. Dyson, *Organometallics* **2006**, *25*, 756–765; e) B. Serli, E. Zangrando, T. Gianferrata, C. Scolaro, P. J. Dyson, A. Bergamo, E. Alessio, *Eur. J. Inorg. Chem.* **2005**, 3423–3434; f) D. N. Akbayeva, L. Gonsalvi, W. Oberhauser, M. Peruzzini, F. Vizza, P. Brügeller, A. Ramerosa, G. Sava, A. Bergamo, *Chem. Commun.* **2003**, 264–265.
[30] D. J. Darensbourg, F. Joo, M. Kannisto, A. Katho, J. H. Reibenspies, D. J. Daigle, *Inorg. Chem.* **1994**, *33*, 200–208.
[31] R. Raveendran, S. Pal, *Polyhedron* **2005**, *24*, 57–63.
[32] B. J. Frost, S. B. Miller, K. O. Rove, D. M. Pearson, J. D. Korinek, J. L. Harkreader, C. A. Mebi, J. Shearer, *Inorg. Chim. Acta* **2006**, *359*, 283–288.
[33] A. Romerosa, T. Campos-Malpartida, C. Lidrissi, M. Saoud, M. Serrano-Ruiz, M. Peruzzini, J. A. Garrido-Cárdenas, F. García-Maroto, *Inorg. Chem.* **2006**, *45*, 1289–1298.
[34] B. J. Frost, C. A. Mebi, *Organometallics* **2004**, *23*, 5317–5323.
[35] A. Sreekanth, H.-K. Fun, M. R. P. Kurup, *J. Mol. Struct.* **2005**, *737*, 61–67.
[36] C. R. Kowol, V. B. Arion, B. K. Keppler, unpublished results.
[37] A. K. Nandi, S. Chaudhuri, S. K. Mazumdar, S. Ghosh, *J. Chem. Soc., Perkin Trans. 2* **1984**, 1729–1733.
[38] C. Scolaro, A. Bergamo, L. Brescacin, R. Delfino, M. Cocchietto, G. Laurenczy, T. J. Geldbach, G. Sava, P. J. Dyson, *J. Med. Chem.* **2005**, *48*, 4161–4171.
[39] K. J. Fisher, E. C. Alyea, N. A. Shahnazarian, *Phosphorus, Sulfur, Silicon Relat. Elem.* **1990**, *48*, 37–40.
[40] S-M. Valiahdi, M. A. Jakupec, B. K. Keppler, unpublished results.
[41] M. Stubbs, P. M. J. McSheehy, J. R. Griffiths, C. L. Bashford, *Mol. Med. Today* **2000**, *6*, 15–19.
[42] R. A. Gattenby, R. J. Gillies, *Nat. Rev. Cancer* **2004**, *4*, 891–899.
[43] L. E. Gerweck, S. V. Kozin, S. J. Stocks, *Br. J. Cancer* **1999**, *79*, 838–842.
[44] B. P. Mahoney, N. Raghunand, B. Baggett, R. J. Gillies, *Biochem. Pharmacol.* **2003**, *66*, 1207–1218.
[45] L. E. Gerweck, S. Vijayappa, S. Kozin, *Mol. Cancer Ther.* **2006**, *5*, 1275–1279.
[46] S. V. Kozin, P. Shkarin, L. E. Gerweck, *Cancer Res.* **2001**, *61*, 4740–4743.
[47] C. M. Laurencot, K. A. Kennedy, *Oncol. Res.* **1995**, *7*, 371–379.
[48] L. E. Gerweck, K. Seetharaman, *Cancer Res.* **1996**, *56*, 1194–1198.
[49] L. F. Tietze, T. Feuerstein, *Curr. Pharm. Des.* **2003**, *9*, 2155–2175.
[50] C. S. Allardyce, P. J. Dyson, D. J. Ellis, S. L. Heath, *Chem. Commun.* **2001**, 1396–1397.
[51] D. L. Klayman, J. P. Scovill, J. F. Bartosevich, C. J. Mason, *J. Med. Chem.* **1979**, *22*, 1367–1373.
[52] D. J. Daigle, *Inorg. Synth.* **1998**, *32*, 40–45.
[53] I. P. Evans, A. Spencer, G. Wilkinson, *J. Chem. Soc., Dalton Trans.* **1973**, 204–209.
[54] W. C. Barette Jr, H. W. Johnson Jr, D. T. Sawyer, *Anal. Chem.* **1984**, *56*, 1890–1898.
[55] Z. Szakacs, G. Hägele, R. Tyka, *Anal. Chim. Acta* **2004**, *522*, 247–258.
[56] *KALEIDAGRAPH*, version 4.03, Synergy Software, Reading, PA, **2006**.
[57] A. Krezel, W. Bal, *J. Inorg. Biochem.* **2004**, *98*, 161–166.
[58] M. R. Pressprich, J. Chambers, *SAINT + Integration Engine, Program for Crystal Structure Integration*, Bruker Analytical X-ray systems, Madison, USA, **2004**.
[59] G. M. Sheldrick, *SHELXS-97, Program for Crystal Structure Solution*, University of Göttingen, Germany, **1997**.
[60] G. M. Sheldrick, *SHELXL-97, Program for Crystal Structure Refinement,* University of Göttingen, Germany, **1997**.
[61] C. K. Johnson, Rep. ORLN-5138, Oak Ridge National Laboratory, Oak Ridge, TN, **1976**.
[62] *International Tables for X-ray Crystallography* (Ed.: A. J. C. Wilson), Kluwer Academic Press, Dordrecht, The Netherlands, **1992**, vol. C, Tables 4.2.6.8 and 6.1.1.4.

Received: December 18, 2006
Published Online: May 22, 2007

